

UPCommons

Portal del coneixement obert de la UPC

<http://upcommons.upc.edu/e-prints>

Aquesta és una còpia de l'author's final draft d'un article publicat a *Energy and Buildings*.

URL d'aquest document a UPCommons E-prints:

<http://hdl.handle.net/2117/116689>

Article publicat / *Published paper*:

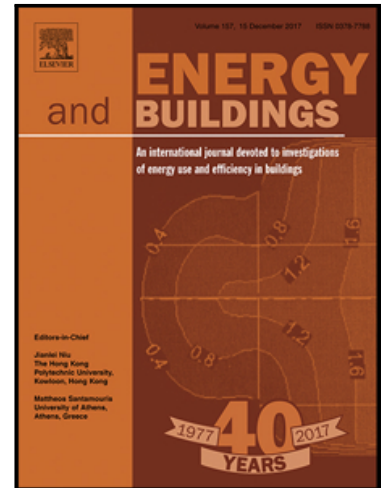
Tejedor ,B., Casals, M., Gangoells ,M. Assessing the influence of operating conditions and thermophysical properties on the accuracy of in-situ measured U-values using quantitative internal infrared thermography. A: *Energy and Buildings* (2018), DOI: <[10.1016/j.enbuild.2018.04.011](https://doi.org/10.1016/j.enbuild.2018.04.011)>.

Accepted Manuscript

Assessing the influence of operating conditions and thermophysical properties on the accuracy of in-situ measured U-values using quantitative internal infrared thermography*

Blanca Tejedor , Miquel Casals , Marta Gangoellis

PII: S0378-7788(17)34029-X
DOI: [10.1016/j.enbuild.2018.04.011](https://doi.org/10.1016/j.enbuild.2018.04.011)
Reference: ENB 8484



To appear in: *Energy & Buildings*

Received date: 11 December 2017
Revised date: 25 February 2018
Accepted date: 5 April 2018

Please cite this article as: Blanca Tejedor , Miquel Casals , Marta Gangoellis , Assessing the influence of operating conditions and thermophysical properties on the accuracy of in-situ measured U-values using quantitative internal infrared thermography*, *Energy & Buildings* (2018), doi: [10.1016/j.enbuild.2018.04.011](https://doi.org/10.1016/j.enbuild.2018.04.011)

This is a PDF file of an unedited manuscript that has been accepted for publication. As a service to our customers we are providing this early version of the manuscript. The manuscript will undergo copyediting, typesetting, and review of the resulting proof before it is published in its final form. Please note that during the production process errors may be discovered which could affect the content, and all legal disclaimers that apply to the journal pertain.

Highlights

- Research was undertaken in an experimental room and real built environments
- Measured U-values were significantly related to outer air temperatures
- The optimum temperature difference ranges between 7 and 16°C
- Heavy multi-leaf walls had more reliable measured U-values at low ΔT ($<7^{\circ}\text{C}$)
- Deviations (0.20%) were smaller for heavy multi-leaf walls with high kappa values

ACCEPTED MANUSCRIPT

Assessing the influence of operating conditions and thermophysical properties on the accuracy of in-situ measured U-values using quantitative internal infrared thermography*

Blanca Tejedor^{a*}, Miquel Casals^a, Marta Gangoellés^a

^a Universitat Politècnica de Catalunya, Department of Project and Construction Engineering, Group of Construction Research and Innovation (GRIC), C/ Colom, 11, Ed. TR5, 08222 Terrassa (Barcelona), Spain

*Corresponding author: Blanca Tejedor. Tel: (+34) 93 7398919, Fax: (+34) 93 7398101.
E-mail: blanca.tejedor@upc.edu

Abstract

Within the European context, most of the current residential building stock does not fulfil minimum thermal requirements and needs to be refurbished urgently. Quantitative internal infrared thermography can provide valuable information about the in-situ thermal transmittance of existing buildings for their future refurbishment. This paper aims to establish how operating conditions and thermophysical properties might affect the accuracy of the measured U-value using this technique. To assess the most influential operating conditions, one experimental room with a heavy single leaf-wall was chosen to develop the research in quasi steady-state conditions, with a wide temperature difference range ($3.8 < \Delta T < 21^\circ\text{C}$). A statistical analysis demonstrated that the variance in thermal transmittance could mainly be predicted by changes in the outer air temperature. To analyze the impact of the thermophysical properties, specifically the heat capacity per unit of area, four unoccupied residential buildings with heavy multi-leaf walls were tested ($6 < \Delta T < 10^\circ\text{C}$). The results mainly showed that the quantitative internal infrared thermography method is more accurate in heavy multi-leaf walls with high kappa values, reaching maximum deviations of 0.20%.

Keywords: quantitative internal infrared thermography (IRT), measured U-value, in-situ measurement, building façade, real built environment, heavy single-leaf walls, heavy multi-leaf walls, operating conditions, heat capacity per unit of area, kappa value

1. INTRODUCTION

Most of the current European residential stock does not satisfy the minimum thermal specifications [1-4]. Specifically, within the European context, over 40% of buildings were built before 1960 and 90% before 1990, and most of them will still be standing in 2050 [1, 5-8]. This implies that up to 110 million buildings need refurbishment [7]. Unfortunately, the renovation rate across the EU is estimated to be very low, at around 1% per year [1, 5-7, 9, 10]. Nowadays, most of the energy efficiency measures are focused on maximizing the thermal performance of components [11]. The requirements in the regulations on façades have grown and are expected to continue growing in the future [12]. In general, construction project documents are not available for existing buildings, especially the oldest ones, but methods such as quantitative internal infrared thermography (IRT) can provide valuable information about in-situ thermal transmittance of the façade for future refurbishment [13]. To guarantee correct execution of in-situ quantitative IRT tests and accurate outcomes, some operating conditions must be fulfilled. Previous researchers stated that tests must be performed under 10-15°C of temperature difference between outside and inside the building to ensure measurable heat exchange across the building envelope [14- 22], although this parameter could be reduced to a lower level ($7 < \Delta T < 16^{\circ}\text{C}$) according to Tejedor et al. [13].

Accuracy in the determination of the thermal behavior of façades [23] and the influence of operating conditions [24] have become a widely discussed concern in recent years, regardless of the technique used for the assessment (i.e. heat flux meter –HFM-, guarded hot box, and quantitative infrared thermography, among others). For quantitative external IRT, some authors proposed a sensitivity analysis in relation to the deviation between the theoretical and measured U-values. Lehman et al. [25] quantified the influence of climatic conditions on the surface temperature distribution in both insulated and non-insulated façades by simulations in transient regime, to derive a criterion for IRT measurements. External wall surface temperature strongly depended on wall assembly, thermal properties of materials and solar irradiation. Tzifa et al. [26], Albatici et al. [27] and Nardi et al. [28] analyzed the influence of variables such as wind speed, outer and inner air temperatures and external wall surface temperature on the accuracy of U-values

in steady-state conditions. Errors depended on the thermal mass and on the exposure of the wall, while wind speed was negligible for heavy walls. In addition, Albatici et al. [27] concluded that a deviation of 50% in the determination of outer air temperature and wall surface temperature could lead to deviations from 50% (heavy walls) up to 350% (light walls) when U-values were measured by IRT. This was attributed to the use of different measuring equipment (an IR camera versus a thermo hygrometer) for low temperature values (0°C). In this case, tests were performed in an experimental building designed for the research with five wall types.

Far fewer studies have been undertaken on quantitative internal IRT. Fokaides et al. [15] drew up a sensitivity analysis, focused on the parameters required to determine the wall surface temperature with an IR camera. Results showed that the most sensitive parameters were the reflected ambient temperature and the assumed emissivity of the wall surface. For instance, a deviation of 1°C in the determination of the reflected ambient temperature might lead to an error of up to 10% in the wall surface temperature. Consequently, this might convert into a deviation of 100% in the determination of U-value [15]. Nardi et al. [24] analyzed the four approaches proposed in the last few years [29, 15, 17, 27] in a single sample by guarded hot box. Measured U-values were plotted against the temperature difference, the reflected ambient temperature and the outdoor temperature difference. Outcomes showed better estimations of thermal transmittances for lower reflected ambient temperatures when the temperature difference increased.

As mentioned above, some authors highlighted the role of walls' thermal mass on the accuracy of measured thermal transmittances for $10 < \Delta T < 15^\circ\text{C}$. However, their studies were conducted on laboratories or experimental rooms using quantitative external IRT, HFM and simulation among other techniques [14, 17, 25-28]. U-value uncertainties provided by HFM depend on the measurement conditions that are registered, the building envelope (light or heavy wall), the data analysis (average method, black box method, LORD, among others) and the HFM' equipment [30, 27, 31]. In accordance with research carried out by Rabadiya et al. [32], the HFM can only measure a local point on the wall, and consequently it does not provide accurate results for non-homogeneous building elements. Regarding quantitative internal IRT, the influence of thermophysical properties on the accuracy of the method has not been addressed in the literature. In terms of thermal behavior of the façade, European regulation

UNE-EN ISO 13786:2011 [33] introduced several thermal parameters for building envelopes (in addition to thermal transmittance), as well as their calculation procedures. Nevertheless, most are transient parameters that can be used to describe the dynamic behavior of the elements [34]. They include thermal time shift, thermal decrement factor and periodic thermal transmittance. The only non-transient thermal parameters that might explain different accuracy values in heavy multi-leaf walls under the same operating conditions are the heat capacity per unit of area and the thermal transmittance. Normally, the effects of thermal inertia and heat capacity per unit of area (kappa value) are not considered, because data are acquired by instantaneous measurements [24]. Hence, it might be interesting to observe whether some of the aforementioned thermophysical properties should be included as a source of inaccuracy when quantitative internal IRT is implemented in real built environments, especially unoccupied buildings where ΔT is $<10^{\circ}\text{C}$.

Within this context, the aim of this paper is to analyze the influence of operating conditions and thermophysical properties that might affect the accuracy of in-situ measured U-values using quantitative internal IRT. For this reason, the paper is based on implementation of the method proposed by Tejedor et al. [13] in several measurement campaigns. Firstly, to evaluate the influence of operating conditions on the measured U-value, an experimental room with a heavy single-leaf wall was tested under a wide temperature difference range ($3.8 < \Delta T < 21^{\circ}\text{C}$). Subsequently, data were statistically assessed. In a second step, once the most significant operating conditions had been determined, the impact of thermophysical properties (heat capacity per unit of area and thermal transmittance) was evaluated in several real built environments with typical heavy multi-leaf walls in relation to the accuracy of the method. Considering that the method was executed in quasi steady-state conditions, dynamic thermal parameters of the walls (i.e. thermal time shift, thermal decrement factor and periodic thermal transmittance) were not analyzed.

Notably, standardized methods (i.e.HFM) were not applied to validate the results, since all tests were performed on heavy façades. Some researchers demonstrated a low discrepancy (1.3-2.6%) between the measured U-values obtained by HFM and the IRT for heavy walls, in contrast to light walls that reached discrepancies of 47.6% [28, 35]. However, light walls (i.e. wood-frame insulated walls or walls with a heat capacity per unit of area lower than $150 \text{ kJ/m}^2 \cdot \text{K}$) are not erected generally in Spain.

The paper is divided into the following sections. Section 2 briefly outlines the main aspects of the quantitative internal infrared thermography method used in this research, which is fully developed in Tejedor et al. [13]. Section 3 describes the research methodology used in this paper. Section 4 discusses the results in depth and assesses the influence of operating conditions and thermophysical properties on the accuracy of measured U-values. Finally, Section 5 highlights the major contributions of this research.

2. QUANTITATIVE INTERNAL INFRARED THERMOGRAPHY

The theoretical framework of the numerical model used in this paper to determine the in-situ measured U-value, and to evaluate accuracy and uncertainty, is extensively reported in Tejedor et al. [13]. Hence, this section only briefly sets out the main equations and the measuring equipment needed to implement the method.

Assuming one-dimensional and horizontal heat flux under steady-state conditions through the building façade, the instantaneous measured U-values can be determined by Equation 1:

$$U_{mes_i} = \frac{(q_c + q_r)}{(T_{IN} - T_{OUT})} = \frac{\left\{ 0.825 + \frac{0.387 \cdot Ra^{\frac{1}{6}}}{\left[1 + \left(\frac{0.492}{Pr} \right)^{\frac{9}{16}} \right]^{\frac{8}{27}}} \right\} \cdot \lambda_{air}}{L} \cdot [T_{IN} - T_{WALL}] + \varepsilon_{WALL} \cdot \sigma \cdot [T_{REF}^4 - T_{WALL}^4] \quad (1)$$

Where U_{mes_i} [W/ (m²·K)] is the sum of the instantaneous specific heat fluxes through the building envelope by convection q_c [W/m²] and radiation q_r [W/m²], divided by the temperature difference (ΔT) between inside and outside the building [K]. Hence, T_{IN} denotes the inner air temperature [K] and T_{OUT} refers to the outer air temperature [K]. Other parameters in the equation are: the wall surface temperature (T_{WALL}) in [K]; the reflected ambient temperature (T_{REF}) in [K]; the emissivity of the wall (ε_{WALL}) that is established as 0.88 for gypsum plaster; Stefan–Boltzmann's constant (σ) with a value of 5.67×10^{-8} [W/m²·K⁴]; the thermal conductivity of the air ($\lambda_{air} = 0.024$ W/m·K for $T_{IN} = 0-15^\circ\text{C}$ and $\lambda_{air} = 0.025$ W/m·K for $T_{IN} = 15-25^\circ\text{C}$); the height of the wall (L) seen from inside the building and expressed in meters; and the dimensionless parameters Rayleigh (Ra) and Prandtl (Pr) numbers. As regards the Prandtl number, it can

be assumed to be 0.73 for $T_{IN}=0-25^{\circ}\text{C}$. However, the Rayleigh number (Equation 2) should be calculated, since it mainly depends on the inner air temperature (T_{IN}) and the wall surface temperature (T_{WALL}):

$$Ra = G_r \cdot Pr = \frac{g \cdot \beta \cdot (T_{IN} - T_{WALL}) \cdot L^3}{\nu^2} \cdot Pr \quad (2)$$

Where G_r is the Grashof number; g refers to gravitation (9.8 m/s^2); β is the volumetric temperature expansion coefficient [$1/\text{K}$] that is defined by $\beta=1/T_m$, where $T_m = (T_{IN} + T_{WALL})/2$; ν is the air viscosity with a value of $1.4 \cdot 10^{-5} \text{ m}^2/\text{s}$ for $T_{IN}= 0-15^{\circ}\text{C}$ and $1.5 \cdot 10^{-5} \text{ m}^2/\text{s}$ for $T_{IN}=15-25^{\circ}\text{C}$.

Notably, operating conditions referring to environmental parameters (T_{IN} and T_{OUT}) are measured and recorded by data loggers with type K thermocouples (TF-500, PCE -T390, PCE Iberica SL), with a resolution of 0.1°C and accuracy of $\pm 0.4\% +0.5^{\circ}\text{C}$. In contrast, parameters relating to the building envelope (ε_{WALL} , T_{REF} and T_{WALL}) are monitored using a reflector, a blackbody and an IR camera of long wavelength band ($7-13 \mu\text{m}$ of the spectral range). Both reflector and blackbody are required to calibrate the IR camera in relation to the wall and compensate the errors of reading. The reflector, which provides the average temperature of the surroundings considering the different reflection indexes (also denoted as T_{REF} -reflected ambient temperature-), is a crinkled piece of aluminium foil with dimensions 0.20×0.15 meters. The blackbody, that allows establishing the wall surface emissivity (ε_{WALL}), is a black tape with dimensions 0.01×0.05 meters and an emissivity of 0.95. Another type of a blackbody (i.e. a smoked metallic sheet) has been rejected, because it does not achieve the target surface temperature. The thermal camera is FLIR60bx (FLIR SYSTEMS), characterized by a field of view of $25 \times 19^{\circ}$, an IR resolution of 320×240 pixels (thermal sensitivity $<0.045^{\circ}\text{C}$ at 30°C) and an accuracy of $\pm 2^{\circ}\text{C}$ or 2% reading at ambient temperature (10 to 35°C). Post-processing of thermograms is carried out by means of FLIR TOOLS + software [36].

Once all instantaneous measured U-values ($U_{mes\ i}$) have been determined, Equation 3 is applied to obtain the average measured U-value [$\text{W}/(\text{m}^2 \cdot \text{K})$]:

$$U_{mes\ avg} = \frac{\sum_{i=1}^n U_{mes\ i}}{n} \quad (3)$$

Where n denotes the total number of thermograms that are assessed for the test.

To evaluate the accuracy of in-situ measurements, a comparison of the measured U-value with the theoretical U-value (U_t) is required. Nominal design data is determined according to construction project documents, the specifications of manufacturers, and the technical data available in the Spanish Technical Building Code CTE-DB-HE1 [37] and European Standards, such as UNE-EN ISO 10456:2012 [38] and UNE-EN ISO 6946:2012 [39]. The estimation of the theoretical U-value and its respective deviation with the average measured U-value for each building envelope can be determined by Equations 4 and 5:

$$U_t = \frac{1}{R_t} = \frac{1}{R_{Si} + \sum_{i=1}^n \frac{\Delta x_i}{\lambda_i} + R_{Se}} = \frac{1}{0.13 + \sum_{i=1}^n \frac{\Delta x_i}{\lambda_i} + 0.04} \quad (4)$$

$$\Delta U/U_t = [(U_{mes\,avg} - U_t)/U_t] \cdot 100 \quad (5)$$

Where U_t [$W/(m^2 \cdot K)$] is the theoretical thermal transmittance; $\Delta U/U_t$ [%] is the deviation between the theoretical and the average measured U-value; R_t is the theoretical thermal resistance [$(m^2 \cdot K)/W$]; R_{Si} refers to the theoretical thermal resistance from inside the building and is equal to $0.13 \, m^2 \cdot K/W$; R_{Se} denotes the theoretical thermal resistance from outside the building with a value of $0.04 \, m^2 \cdot K/W$; Δx_i is the thickness of the layer in metres; and λ_i is the thermal conductivity of the layer [$W/(m \cdot K)$].

In accordance with ISO/IEC Guide 98-3: 2008 [40] and considering the accuracy of the equipment (sensors and infrared camera) provided by the manufacturers, the combined standard uncertainty of measurements is assessed by Equation 6:

$$(\sigma U_{mes})^2 = \left(\frac{\delta U_{mes}}{\delta T_{IN}}\right)^2 \cdot (\sigma T_{IN})^2 + \left(\frac{\delta U_{mes}}{\delta T_{OUT}}\right)^2 \cdot (\sigma T_{OUT})^2 + \left(\frac{\delta U_{mes}}{\delta T_{WALL}}\right)^2 \cdot (\sigma T_{WALL})^2 + \left(\frac{\delta U_{mes}}{\delta T_{REF}}\right)^2 \cdot (\sigma T_{REF})^2 + \left(\frac{\delta U_{mes}}{\delta \varepsilon_{WALL}}\right)^2 \cdot (\sigma \varepsilon_{WALL})^2 \quad (6)$$

Where σT_{IN} and σT_{OUT} are the uncertainties associated with the environmental indoor and outdoor temperature measuring equipment respectively. σT_{WALL} , σT_{REF} and $\sigma \varepsilon_{WALL}$ are the uncertainties associated with the infrared camera when the wall surface temperature, the reflected ambient temperature and the wall emissivity are measured respectively.

3. RESEARCH METHODOLOGY

The research methodology used in this paper includes two main steps that are fully described in Section 3.1 (Analysis of the most influential operating conditions) and 3.2. (Analysis of the influence of thermophysical properties).

3.1. Analysis of the most influential operating conditions

To determine the most influential operating conditions, several temperature difference ranges were assessed for the same U-value, using the method developed by Tejedor et al. [13]. The measurement campaign, which took place during January and February 2016, was performed on an experimental room located in the university with a heating unit to be configured (Figure 1). The façade consisted of a single-leaf wall of 3.26 m height with a theoretical U-value of $2.310 \text{ W/m}^2 \cdot \text{K}$, since it was erected before NBE-CT-79 [41] without any subsequent refurbishment. As regards its internal configuration (from outside to inside), this building envelope is comprised of 20 mm of mortar, 140 mm of perforated brick wall and 10 mm of gypsum plaster. A total of 966 thermograms were recorded to assess the thermal behavior of this façade for an air temperature difference range from 3.80 to 20.60°C between inside and outside the building and to determine the optimum temperature difference range for quantitative internal IRT. Measured U-values, with their respective deviations and combined standard uncertainties associated with the measuring equipment, were calculated following the quantitative internal IRT method described in Tejedor et al. [13], and briefly summarized in Section 2 of this paper (Equations 1 to 6).

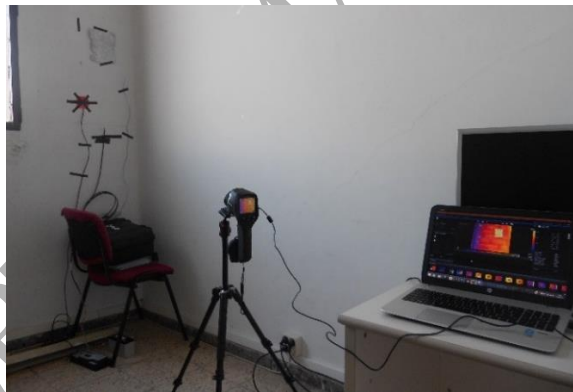


Figure 1. Experimental room

For the in-depth analysis, the main operating conditions to be evaluated were those continuously measured by the equipment and introduced as input data in the numerical model. Considering this premise, and in accordance with the method proposed by the authors, the analyzed parameters were as follows: temperature difference (ΔT), inner air temperature (T_{IN}), outer air temperature (T_{OUT}), wall surface temperature (T_{WALL}) and reflected ambient temperature (T_{REF}). However, the wall surface emissivity (ε_{WALL}) was not considered as a possible causal factor of deviation in this research, since

Tejedor et al. [13] already demonstrated that measurements are slightly influenced by this parameter. To identify a significant relationship between these variables and the measured U-value, a statistical analysis based on Pearson's correlation was computed using SPSS Statistics Software [42].

3.2. Analysis of the influence of thermophysical properties

Having identified the most influential operating conditions and the optimum temperature difference range, the second step of the methodology was to assess the influence of the walls' thermophysical properties on the accuracy of the measured U-value. In this case, the measuring campaign was conducted in unoccupied residential buildings (Façades 1 to 4) from January to February 2017, to ensure the same internal boundary conditions among samples and similar external weather conditions to the first step of the research. These unoccupied buildings form part of public housing stock and have no electric or heating system in operation. In fact, some of them (Façades 2, 3 and 4) have not been in-use since they were built. In the case of Façade 1, the housing had not been occupied for years, since it needed to be refurbished in accordance with current regulations. Hence, stable environmental conditions were maintained before testing. During the performance of the method, the doors and windows remained closed.

Façades 1 (Figure 2) and 2 were erected under NBE-CT-79 [41], while Façades 3 (Figure 3) and 4 were built under the Spanish Technical Building Code CTE-DB-HE1 [37]. To evaluate deviation of the measured U-values in relation to the thermophysical properties, a sequential video of 121 thermograms was recorded for each wall. Table 1 shows the configuration and the main technical features of the four analyzed façades. Notably, endoscopy analyses could not be performed. The thicknesses of each layer were taken from the construction project documents. Concerning other technical features of façades, some construction project documents provided the thermal resistances of each layer. Other documents contained the conductivities and thermal resistances of each layer of the wall, and even the manufacturers' datasheets. Values of density and specific heat capacity were taken from UNE-EN ISO 10456:2012 [38] and the existing literature [14, 43, 34]. The theoretical thermal resistance from inside the building (R_{si}) and the theoretical thermal resistance from outside the building (R_{se}) were taken from the technical data available in the Spanish Technical Building Code CTE-DB-HE1 [37]. To calculate the theoretical U-value, UNE-EN ISO 6946:2012 [39] was applied.



Figure 2. Measuring campaign in Façade 1



Figure 3. Measuring campaign in Façade 3

Table 1. Configuration and technical features of the façades (from outside to inside)

	N#	Material	Δx_i	λ_i	ρ_i	$c_{p i}$	$R_{t i}$	L	U_t
	layer	layer	[m]	[W/(m·K)]	[kg/m ³]	[J/(kg·K)]	[(m ² ·K)/W]	[m]	[W/(m ² ·K)]
Façade 1	1	Perforated brick wall	0.140	---	1140	1000	0.180		
	2	Insulation EPS	0.030	0.033	30	1400	0.909		
	3	Non-ventilated air cavity	0.020	---	1	1004	0.160	2.50	0.657
	4	Hollow brick wall	0.050	---	1000	1000	0.070		
	5	Gypsum plaster	0.010	0.300	1150	1000	0.033		
Façade 2	1	Insulation EPS	0.080	0.038	20	1400	2.125		
	2	Perforated brick wall	0.140	---	1140	1000	0.180		
	3	Non-ventilated air cavity	0.050	---	1	1004	0.180	2.70	0.362
	4	Hollow brick wall	0.040	---	1000	1000	0.090		
	5	Gypsum plaster	0.010	0.570	1150	1000	0.018		
Façade	1	Limestone wall	0.030	2.300	2395	920	0.013		0.480

3	2	Reinforced concrete wall	0.250	2.300	2400	1000	0.109	2.51	
	3	Rock wool insulation	0.064	0.037	40	840	1.730		
	4	Plasterboard	0.016	0.250	825	1000	0.064		
Façade	1	Mortar	0.002	1.300	1900	1000	0.002		
	2	Insulation EPS	0.060	---	20	1400	1.620		
	4	Thermoclay	0.240	---	910	719	0.570	2.54	0.420
	4	Gypsum plaster	0.010	0.570	1150	100	0.018		

Δx_i : thickness of the layer; λ_i : thermal conductivity of the layer; ρ_i : density of the layer; c_{pi} : specific heat capacity of the layer; $R_{t,i}$: theoretical thermal resistance of the layer; L : height of the wall; U_i : theoretical thermal transmittance of the building façade.

In contrast to the operating conditions, the thermophysical properties include aspects of the building envelope which cannot be controlled by the thermographer, but might also influence the accuracy of the quantitative internal IRT. Considering that the method proposed by Tejedor et al. [13] was executed in quasi steady-state conditions, measured U-value and theoretical heat capacity per unit of area of each façade were the only non-transient thermophysical properties to be considered in this research. Measured U-values were determined following Section 2 of this paper (Equations 1 to 5). Heat capacity per unit of area (also referred to as the kappa value or k_m) defines the quantity of heat to be stored by an element for later release and characterizes the thermal mass [31]. Hence, a wall with a high potential to accumulate heat has a high thermal mass. According to UNE-EN ISO 13786:2011 [33], the theoretical heat capacity per unit of area (k_m) can be calculated by Equation 7 (considering that the summation is over all layers in the element).

$$k_m = (\sum \Delta x_i \cdot \rho_i \cdot c_{pi}) / 1000 \quad (7)$$

Where k_m [kJ/m²·K] is the theoretical heat capacity per unit of area; Δx_i is the thickness of the layer [m]; ρ_i is the density of the layer [kg/m³]; and c_{pi} is the specific heat capacity of the layer [J/kg·K].

This simplified method was found to be suitable for this research, since the building envelope can be taken as a plane component and the approximation is not used to define the thermal inertia of the wall. However, it might provide overestimations in comparison to the results obtained from dynamic thermal characteristics.

4. RESULTS AND DISCUSSION

The following subsections discuss the results obtained in steps 1 and 2 of the research methodology.

4.1. Analysis of the most influential operating conditions

Six tests were performed in an experimental room ($U_i=2.310 \text{ W/m}^2\cdot\text{K}$) with a heating unit under quasi steady-state conditions for several temperature difference ranges. Tests took 2-3 hours with a data acquisition interval of 1 minute for each case.

Firstly, the analysis was carried out without heating (Test 1), under a temperature difference between inside and outside the building that ranged from 3.80 to 9.80°C. Just one test was enough to reject this ΔT for the numerical model, since the worst outcomes were gathered for Test 1 with an average measured U-value of $3.618\pm 0.542 \text{ W/m}^2\cdot\text{K}$ (Table 2 and Figure 4). The instantaneous thermal transmittances were found to be overestimated, specifically 140-150% higher than the theoretical value when the temperature difference was around 3°C-4°C. This percentage was reduced to ~100% when ΔT ranged from 4 to 5°C and 60% under 6°C. Subsequently, three tests were conducted for a temperature difference between 7 and 16°C (Tests 2, 3 and 4 in Table 2). The measurements of 543 thermograms were found to better fit the theoretical U-value, with the average measured U-value equal to $2.396\pm 0.304 \text{ W/m}^2\cdot\text{K}$ (deviation of 3.73%). Finally, two tests were performed for $16 < \Delta T < 21^\circ\text{C}$ (Tests 5 and 6 in Table 2), showing similar results. In this case, the average measured thermal transmittance was found to be $2.017\pm 0.194 \text{ W/m}^2\cdot\text{K}$, so was underestimated by 12.66% in relation to the theoretical U-value. Therefore, a third test for this temperature difference range was deemed not to be necessary.

Table 2. Measured U-values using quantitative internal IRT (absolute deviations are presented as percentages)

Measured U-value					
$U_{\text{mes}} [\text{W}/(\text{m}^2\cdot\text{K})]$					
Test 1	Test 2	Test 3	Test 4	Test 5	Test 6
3.80< ΔT < 9.80°C	7.90< ΔT < 14.90°C	6.70< ΔT < 15.30°C	7< ΔT < 15.80°C	16.60< ΔT < 20.40°C	16.50< ΔT < 20.60°C
121 thermograms	181 thermograms	181 thermograms	181 thermograms	121 thermograms	181 thermograms
3.618±0.542		2.396 ±0.304		2.017±0.194	
(56.63%)		(3.73%)		(-12.66%)	

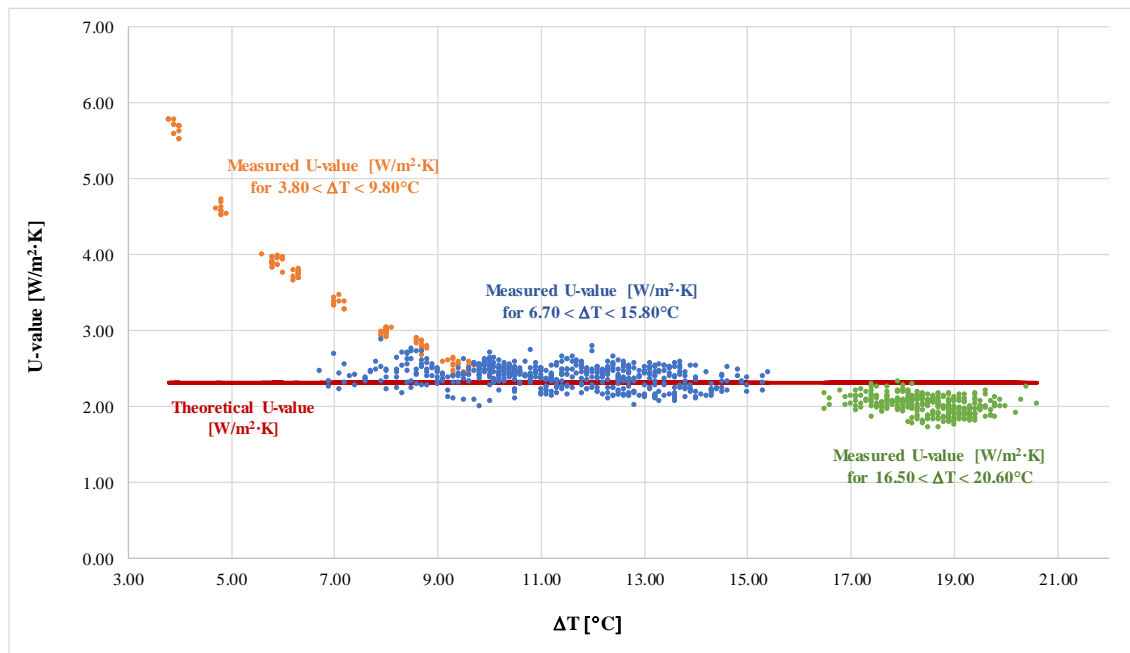


Figure 4. Measured thermal transmittance for $3.80 < \Delta T < 20.60^\circ\text{C}$

As mentioned in Section 3.1., the main operating conditions that might affect the accuracy of measured U-values were those referred to as input data of the numerical model (ΔT , T_{IN} , T_{OUT} , T_{WALL} and T_{REF}). However, temperature difference (ΔT) is an operating condition that derives from two others (the inner and outer air temperatures near the target to be tested). Therefore, both T_{IN} and T_{OUT} should be carefully studied. The statistical analysis of input data was drawn up for each temperature difference range using a t-test analysis, specifically a Pearson's parametric correlation (r-value). A normal distribution at 95% confidence level was assumed in SPSS software [42]. The results are summarized in Tables 3 to 5, where the r^2 value indicates how a variable can be predicted by changes in another one [44, 45]. Notably, the tables provide the r-value. To obtain the percentage of variance in thermal transmittance due to each operating condition, the square value of Pearson's correlation coefficients (r-value) should be calculated and multiplied by 100. Figures 5 to 7 corroborate the results gathered from statistical analysis. These figures illustrate the relationship among the operating conditions and the measured U-values (blue points) with respect to the theoretical U-values (red lines), as temperature differences (ΔT) are sorted and plotted from lowest to highest. In this way, and for the three ΔT ranges evaluated above ($3.80 < \Delta T < 9.80^\circ\text{C}$; $7 < \Delta T < 16^\circ\text{C}$; $16 < \Delta T < 21^\circ\text{C}$), it can be observed the evolution of the input data for the numerical model

(T_{IN} , T_{OUT} , T_{WALL} and T_{REF}) and the adjustment of the measured U-value to the expected value when ΔT increases.

According to the results (Table 3), for a temperature difference range from 3.80 to 9.80°C (Test 1), the thermal transmittance absolutely depends on ΔT ($r=-0.963$) as a direct consequence of outer air temperature near the target ($r=+0.973$). Data showed that 94.67% of the variance in thermal transmittance could be attributed to changes in T_{OUT} , being the percentage of correlation between T_{OUT} and ΔT of 99.40%. As corroborated by Figure 5, T_{OUT} and the measured U-value describe the same decreasing trend when ΔT values increase, whereas other operating conditions (inner air temperature, wall surface temperature and reflected ambient temperature) remain practically constant. The registered values of T_{IN} were around 15°C; T_{WALL} and T_{REF} were remained in 11°C and 14°C respectively. It should be noted that T_{WALL} was found to be the parameter with the least influence on the measured U-value (2.46%), considering results of Table 3.

Table 3. Correlation matrix for measured U-values and operating conditions for $3.80 < \Delta T < 9.80^\circ\text{C}$

	Umes	ΔT	T_{IN}	T_{OUT}	T_{WALL}	T_{REF}
Umes	1					
ΔT	-0.963**	1				
T_{IN}	-0.426**	0.584**	1			
T_{OUT}	0.973**	-0.997**	-0.522**	1		
T_{WALL}	0.157	-0.075	0.468**	0.122	1	
T_{REF}	-0.214*	0.310**	0.674**	-0.264**	0.899**	1

** Correlation is significant at the 0.01 level (2-tailed); $n=121$

* Correlation is significant at the 0.05 level (2-tailed); $n=121$

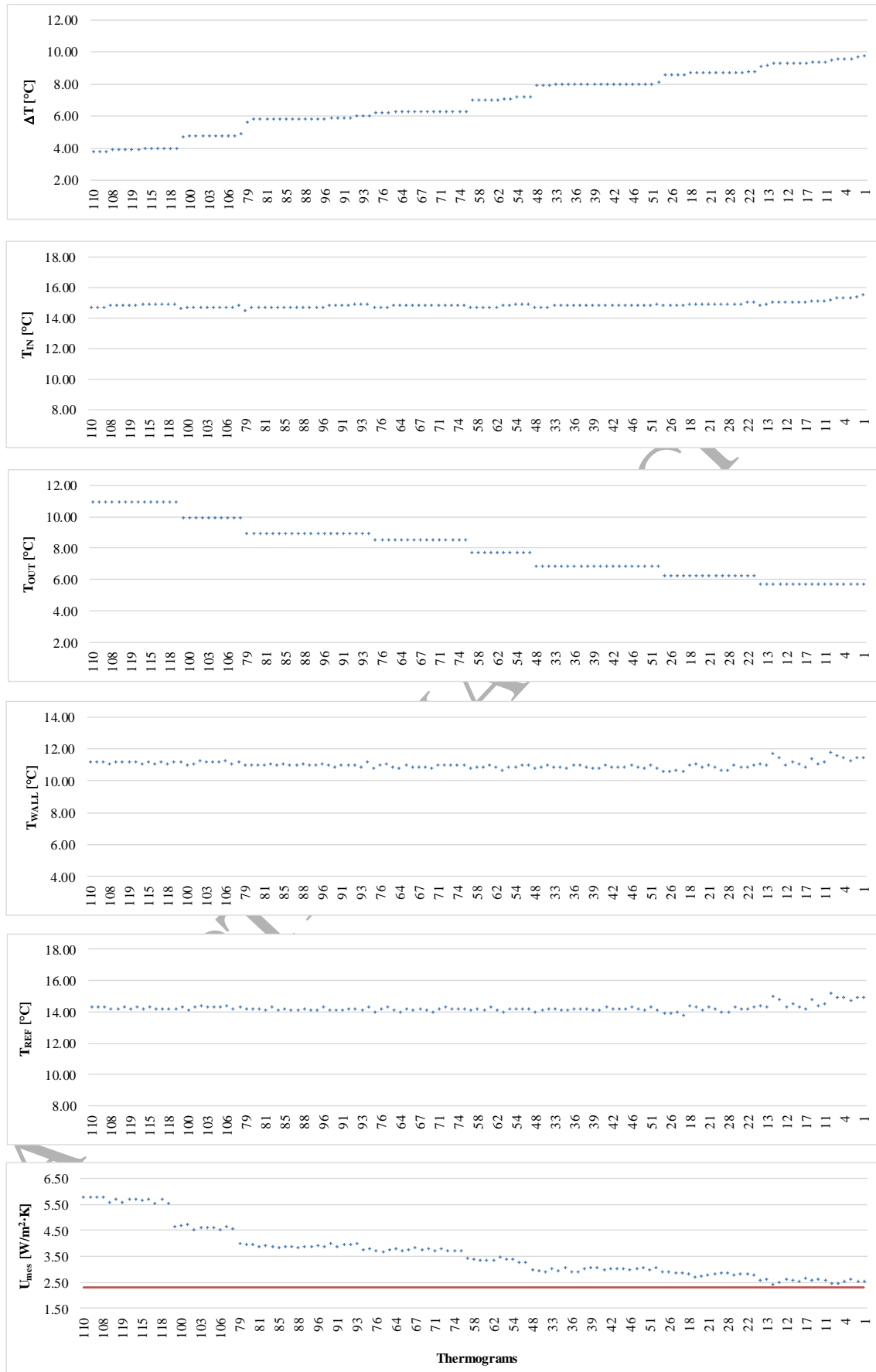


Figure 5. Influence of operating conditions on the measured U-value for $3.80 < \Delta T < 9.80^{\circ}\text{C}$

For a temperature difference range between 7 and 16°C (Table 4 and Figure 6), correlation data revealed that the thermal transmittance was only significantly related to the outer air temperature near to the target ($r=+0.469$). In this case, the r^2 was low, indicating that only 22% approximately of the variance in the measured U-value could be predicted by changes of T_{OUT} . In addition, a negative Pearson's correlation value between ΔT and T_{OUT} ($r=-0.848$) indicated that 71.91% of the variance in ΔT could be caused by decreases in T_{OUT} .

Table 4. Correlation matrix for measured U-values and operating conditions for $7 < \Delta T < 16^\circ\text{C}$

	U_{mes}	ΔT	T_{IN}	T_{OUT}	T_{WALL}	T_{REF}
U_{mes}	1					
ΔT	-0.296**	1				
T_{IN}	0.270**	0.376**	1			
T_{OUT}	0.469**	-0.848**	0.171**	1		
T_{WALL}	0.108*	-0.534**	0.460**	0.830**	1	
T_{REF}	0.077	-0.370**	0.563**	0.714**	0.975**	1

** Correlation is significant at the 0.01 level (2-tailed); $n=543$

* Correlation is significant at the 0.05 level (2-tailed); $n=543$

This analysis did not show any significant relationships between the thermal transmittance and the other operating conditions. As seen in Figure 6, the inner air temperature (T_{IN}), the wall surface temperature (T_{WALL}), and the reflected ambient temperature (T_{REF}) remained practically constant. The majority of datapoints of T_{IN} were from 20 to 22°C throughout the temperature difference range. In the case of T_{WALL} and T_{REF} , the measurements were roughly concentrated between 14-16° for T_{WALL} and 16-18°C for T_{REF} . Besides this, the influences of these three parameters on the measured U-value were very low. Their corresponding r^2 values expressed as a percentage were found to be 7.29%, 1.17% and 0.59% respectively (Table 4).

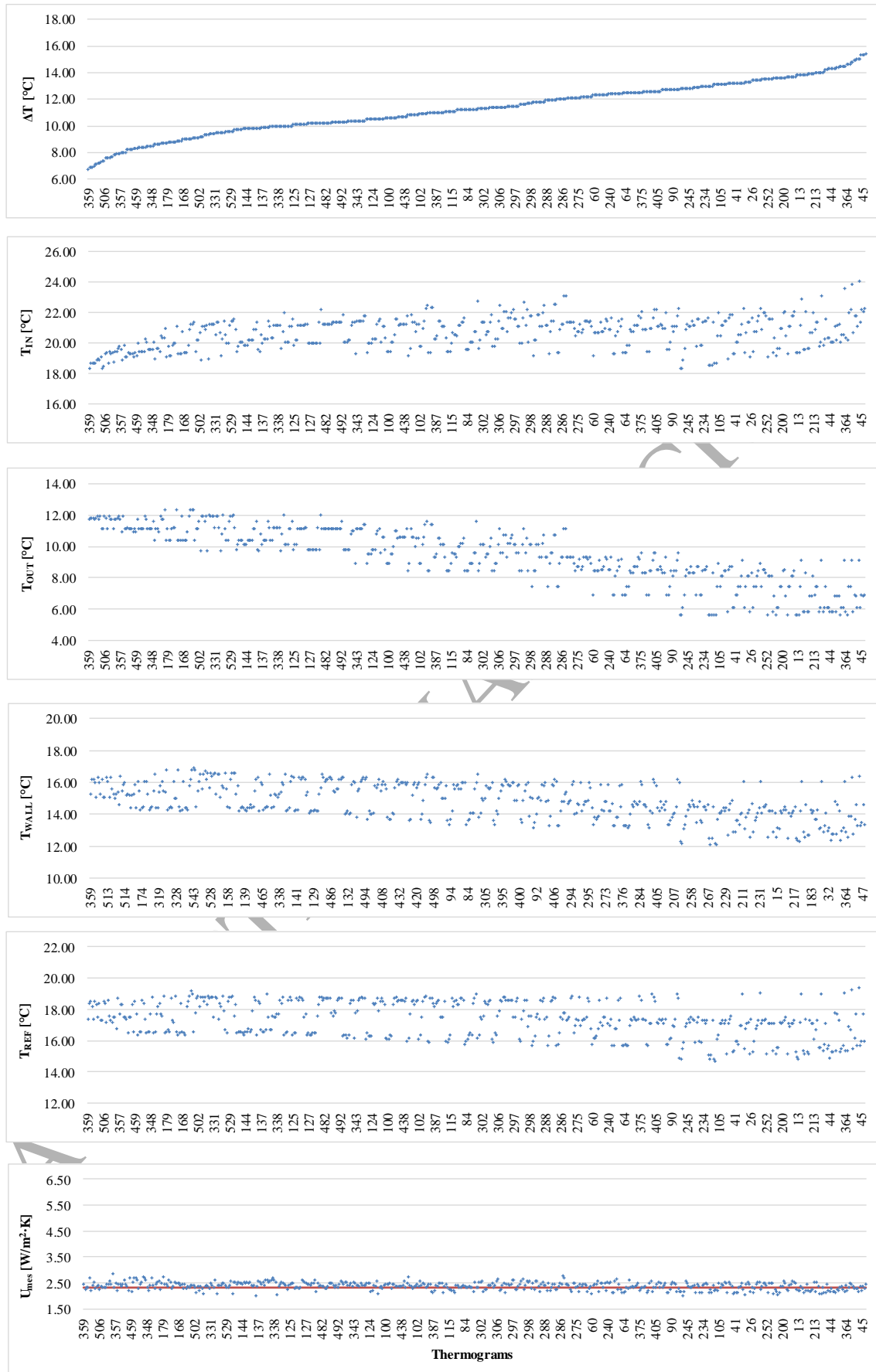


Figure 6. Influence of operating conditions on the measured U-value for $7 < \Delta T < 16^{\circ}\text{C}$

Along the lines of Nardi et al. [24], the findings also showed an underestimation of measured U-value when the temperature difference and reflected ambient temperature increased ($16 < \Delta T < 21^\circ\text{C}$ and $18 < T_{REF} < 20.1^\circ\text{C}$, respectively). All Pearson's coefficients for the measured U-value were found to be negative. In this case (Table 5 and Figure 7), the data showed that 35.64% of the variance of the measured U-values could be predicted by changes in T_{WALL} . In addition, higher correlation coefficients revealed that the majority of T_{WALL} measurements could have been produced by changes in T_{REF} (97.02%) and T_{IN} (80.46%). At higher inner air temperatures, the surroundings (including furniture and white walls) reflect more on the target and consequently might have affected the readings of the wall surface temperature. Wall surface temperatures gathered from 12 to 16°C seemed to be more stable ($14.5 < T_{REF} < 17.9^\circ\text{C}$), giving deviations regarding the theoretical U-value of under $\pm 5\%$. However, a decreasing trend of the measured U-value was observed for $T_{WALL} > 16^\circ\text{C}$, reaching deviations of measured U-values of around -15%.

Table 5. Correlation matrix for measured U-values and operating conditions for $16 < \Delta T < 21^\circ\text{C}$

	U_{mes}	ΔT	T_{IN}	T_{OUT}	T_{WALL}	T_{REF}
U_{mes}	1					
ΔT	-0.352**	1				
T_{IN}	-0.353**	0.876**	1			
T_{OUT}	-0.211**	0.356**	0.763**	1		
T_{WALL}	-0.597**	0.657**	0.897**	0.857**	1	
T_{REF}	-0.468**	0.608**	0.888**	0.905**	0.985**	1

** Correlation is significant at the 0.01 level (2-tailed); $n=302$

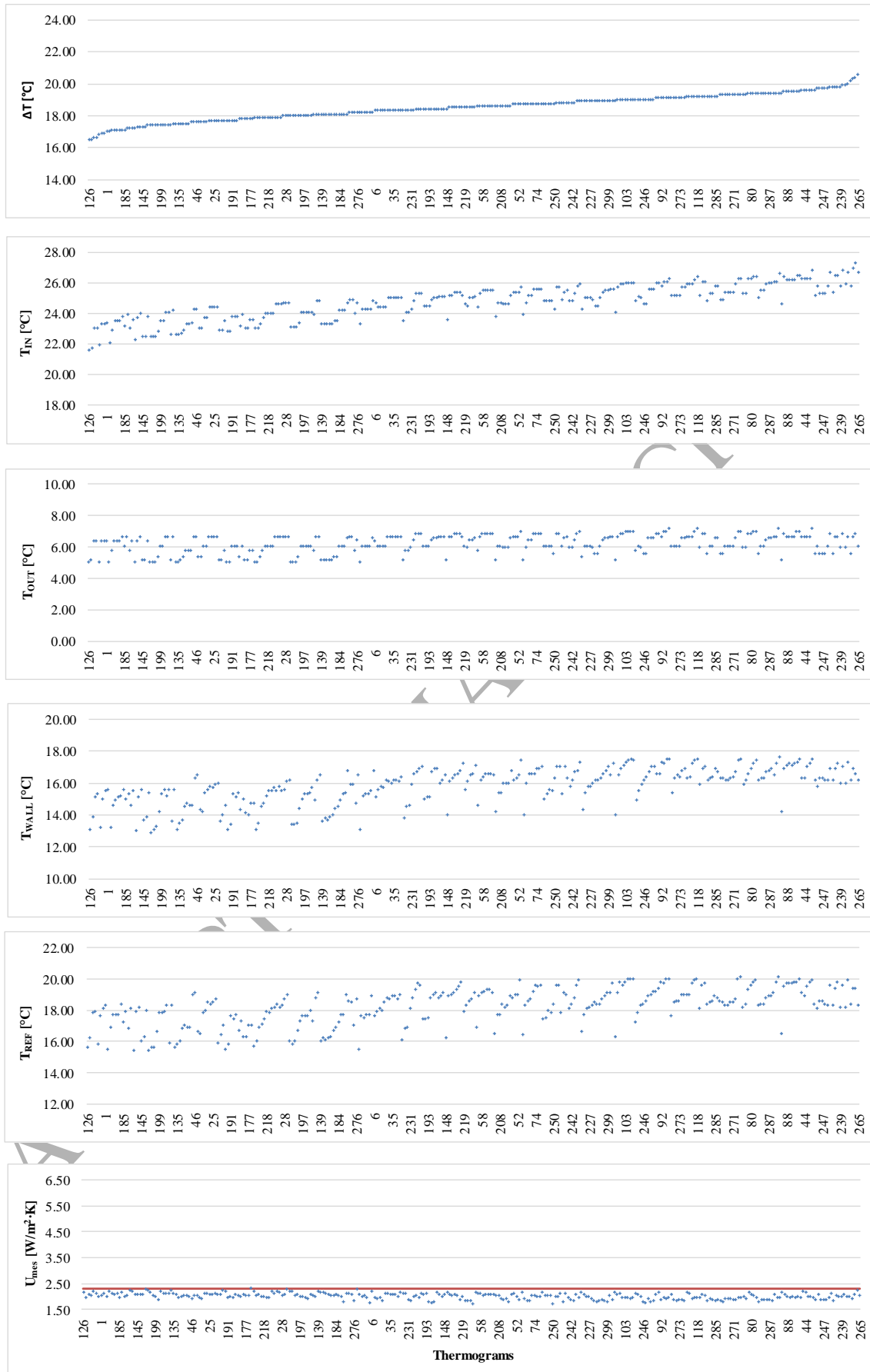


Figure 7. Influence of operating conditions on the measured U-value for $16 < \Delta T < 21^{\circ}\text{C}$

It should be noted that the relationship between T_{WALL} and T_{REF} was observed in the three ΔT ranges, where the measurements of T_{WALL} were highly correlated with T_{REF} . In fact, the reflected ambient temperature is a measurement parameter that is required to compensate errors of wall surface temperature readings with the IR camera. In addition, the percentages of r^2 value for T_{REF} in relation to the variance in thermal transmittance ascended along the wide temperature difference (80.82% for $3.80 < \Delta T < 9.80^\circ\text{C}$; 95.06% for $7 < \Delta T < 16^\circ\text{C}$; 97.02% for $16 < \Delta T < 21^\circ\text{C}$).

Finally, although testing procedures in quasi steady-state conditions might have influenced the variability of some measurements (swinging trend of instantaneous measurements for values of the same order), it can be considered that all obtained outcomes were reliable. A single-leaf wall is quite sensitive to outer air temperature, due to a lack of insulation layer. In addition, a temperature difference range from 7 to 16°C might be considered the optimum.

4.2. Analysis of the influence of thermophysical properties

Four building façades with different heavy multi-leaf wall configurations were evaluated for 2 hours with a data acquisition interval of 1 minute and under the same temperature difference range, roughly from 6 to 10°C in most cases. As can be observed in Table 6, and because of testing in several real built environments, ΔT values were slightly lower than optimal. During the tests, the inner air temperature of the unoccupied buildings remained at $12\text{--}14^\circ\text{C}$ and outside temperatures ranged from 0 and 5°C between 6 am and 9 am. By way of example, the operating conditions and the instantaneous measured U-values were plotted over time in Façade 4 (Figure 8).

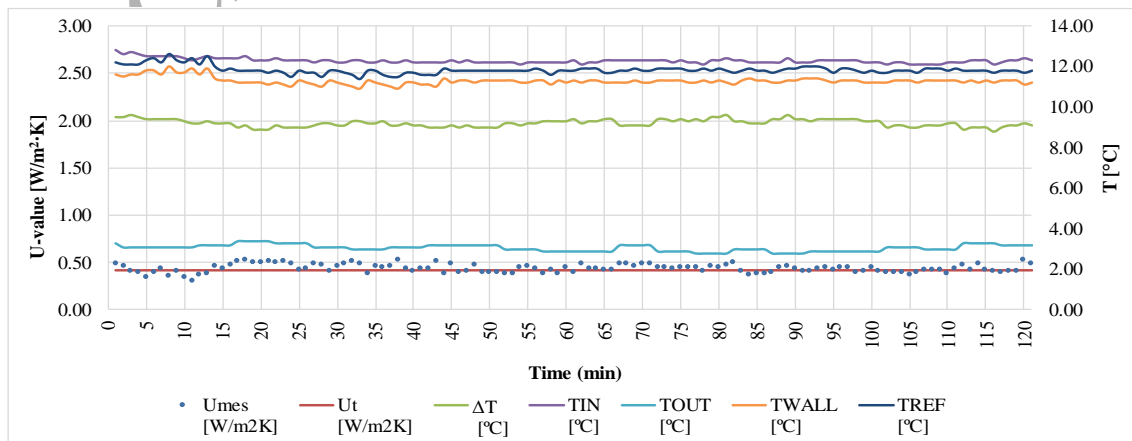


Figure 8. Operating conditions and instantaneous measured U-values over time in Façade 4

As mentioned in Section 3.2, the theoretical heat capacity per unit of area was calculated using UNE-EN ISO 13786:2011 [33] for all building envelopes, according to Equation 7. Aspects such as density and specific heat capacity were estimated following UNE-EN ISO 10456:2012 [38] and some studies developed by other authors [14, 43, 34]. Results are shown in Table 6.

Table 6. Theoretical thermophysical characteristics and measured U-values using quantitative internal IRT (deviations between theoretical and measured U-values are expressed as a percentage)

	Façade 1	Façade 2	Façade 3	Façade 4
	6.8< ΔT < 8.7°C	7.6< ΔT < 9.1°C	5.8< ΔT < 8.2°C	8.70< ΔT < 9.80°C
	121 thermograms	121 thermograms	121 thermograms	121 thermograms
Theoretical Kappa value				
k_m [kJ/(m ² ·K)]	222.38	213.39	685.88	174.01
Theoretical U-value				
U_t [W/(m ² ·K)]	0.657	0.362	0.480	0.420
Measured U-value	0.665±0.214	0.396±0.270	0.481±0.330	0.437±0.219
U_{mes} [W/(m ² ·K)]	(1.19%)	(9.34%)	(0.20%)	(3.97%)

The results lead to the conclusion that heavy multi-leaf walls are less sensitive and provide more reliable results than heavy single-leaf walls for low temperature difference values ($\Delta T < 7^\circ\text{C}$) under quasi steady-state conditions. In general, U-values measured using the proposed method showed deviations under 4% in most samples, except for Façade 2. As shown in Figure 9, where the deviations $\Delta U/U_t$ (%) are plotted against the measured U-value, the percentage of deviation decreased as building envelopes presented greater thermal transmittance. Hence, multi-leaf walls with lower U-values might be more difficult to assess (i.e. Façade 2 had a deviation of 9.34%).

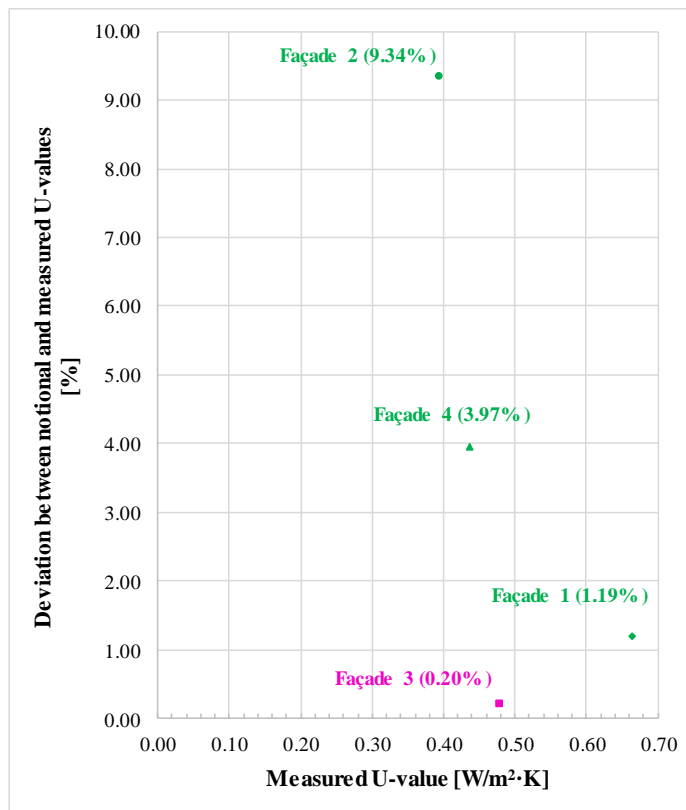
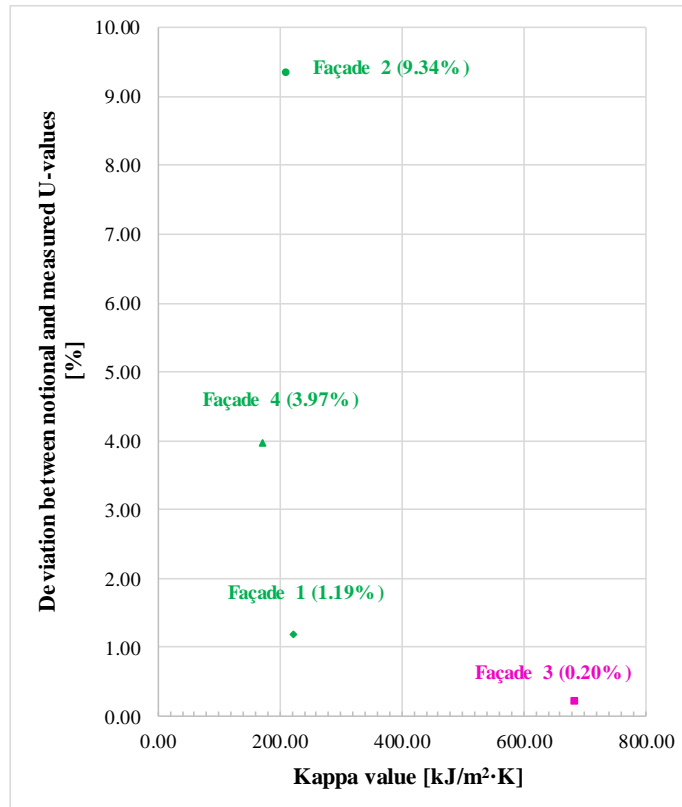


Figure 9. Deviation between the theoretical and measured U-value against the measured U-value

This analysis also demonstrated that façades with high theoretical heat capacities per unit of area might give low deviations (Figure 10), as detailed below. Façades 3 and 4, whose measured thermal transmittances were $0.481 \pm 0.330 \text{ W/m}^2 \cdot \text{K}$ and $0.437 \pm 0.219 \text{ W/m}^2 \cdot \text{K}$, presented deviations of 0.20% and 3.97% respectively (Figure 9). Despite being under the same test conditions, these multi-leaf walls with similar U-values had different accuracy levels in relation to theoretical U-values. In the case of Façade 3, the theoretical heat capacity per unit of area was found to be over 3 times higher than the estimated value for Façade 4 (Figure 10).



Figures 10. Deviation between the theoretical and measured U-value against the Kappa value

5. CONCLUSIONS

The main contribution of this research is the assessment of the influence of operating conditions and thermophysical properties on the accuracy of in-situ measured U-values, using the quantitative internal IRT method. The measuring campaigns were performed in an experimental room and several real built environments.

The research results revealed that the measured U-values were significantly related to the outer air temperature (T_{OUT}) for temperature differences (ΔT) under 16°C . When the inner air temperature increased considerably ($16 < \Delta T < 21^{\circ}\text{C}$), the variance in the measured U-value could be attributed to changes in wall surface temperature (T_{WALL}). The analysis highlighted that the optimum temperature difference range is from 7 to 16°C . Measured U-values were found to be highly overestimated when the temperature difference was around 3 - 4°C and slightly underestimated when ΔT ranged between 16 to 21°C .

For the first time, a study based on internal thermography was undertaken in real unoccupied buildings. The outcomes mainly showed three aspects: (i) multi-leaf walls are less sensitive and provide more reliable results than single-leaf walls for low temperature difference values ($\Delta T < 7^\circ\text{C}$); (ii) quantitative internal IRT is found to be more accurate for multi-leaf walls with high values of heat capacity per unit of area, reaching maximum deviations of 0.20%; (iii) multi-leaf walls with lower U-values might entail deviations of around 9%. These results are consistent with previous studies generally conducted on laboratories or experimental buildings where other techniques were applied.

The findings suggest that quantitative internal IRT might allow the assessment of aspects related to the determination of U-value of unoccupied buildings (without electric and heating systems) for ΔT under 10°C , especially in Spain or European countries with a Mediterranean climate where these test conditions might represent a limitation. Hence, this research increases the applicability range of techniques based on IRT. Nevertheless, further research is required in this area.

This research could also be useful for architects, energy auditors and other stakeholders within the construction industry field, since decision-making could be streamlined in real built environments. Firstly, this research might contribute to avoiding mistakes in relation to operating conditions if quantitative internal IRT was used as a tool for energy audits, at least in European countries with a Mediterranean climate. Secondly, technical staff might be able to estimate the possible deviation of thermal transmittance depending on the wall type to be tested and to check if the measurement is in line with expectations. Possible discrepancies might be related to bad workmanship, a lack of insulation, and ageing of the building materials, among other factors. Therefore, this research might lead to enhanced execution of the refurbishment process in buildings that are expected to have shortcomings in 2050, in accordance with the existing literature. Consequently, it may increase the European renovation rate in the mid-term.

ACKNOWLEDGEMENTS

The authors would like to thank the Industrial Engineers' Institution of Catalonia for financing part of this research through a PhD grant awarded in June 2016. The authors also thank Terrassa City Council for promoting this research through a PhD grant given in December 2016. Finally, the authors express their

gratitude to the Department of Housing and Urban Development of Terrassa for allowing access to Council-owned buildings.

REFERENCES

- [1] Itard and Meijer, 2008. Towards a sustainable Northern European Housing Stock. Figures, facts and future. Available at: < <https://www.arct.cam.ac.uk/Downloads/towards-a-sustainable-northern-european-housing.pdf>> (accessed 31.10.17)
- [2] Dowson, M; Poole, A; Harrison, D; Susman, G. *Domestic UK retrofit challenge: barriers, incentives and current performance leading into the Green Dale*. Energy Policy 50 (2012) 294-305
- [3] Gangoellis, M; Casals, M. *Resilience to increasing temperatures: Residential building stock adaptation through codes and standards*. Building Research & Information 40 (2012) 645-664
- [4] Gangoellis, M; Casals, M; Forcada, N; Macarulla, M; Cuerva, E. *Energy mapping of existing building stock in Spain*. Journal of Cleaner Production 112 (2016) 3895 -3904
- [5] BPIE -Buildings Performance Institute Europe-, 2011. Europe's Buildings Under The Microscope. A country-by-country review of the energy performance of buildings. Available at: < http://bpie.eu/wp-content/uploads/2015/10/HR_EU_B_under_microscope_study.pdf> (accessed 31.10.17)
- [6] EIU –Economist Intelligence Unit-, 2013. Investing in energy efficiency in Europe's buildings. A view from the construction and real estate sectors. Available at: <http://www.gbpn.org/sites/default/files/06.EIU_EUROPE_CaseStudy_0.pdf> (accessed 31.10.17)
- [7] European Parliament's Committee on Industry, Research and Energy [ITRE], 2016. Boosting Building Renovation: What potential and value for Europe. Available at: <[http://www.europarl.europa.eu/RegData/etudes/STUD/2016/587326/IPOL_STU\(2016\)587326_EN.pdf](http://www.europarl.europa.eu/RegData/etudes/STUD/2016/587326/IPOL_STU(2016)587326_EN.pdf)> (accessed 31.10.17)

- [8] Interreg Europe, 2017. Improving energy efficiency in buildings. Available at: <https://www.interregeurope.eu/fileadmin/user_upload/2017-09-11_TO4_policy_brief__EE_in_existing_buildings_v3_KM_kp_final.pdf> (accessed 31.10.17)
- [9] IEA –International Energy Agency-, 2013. Transition to Sustainable Buildings. Strategies and Opportunities to 2050. Available at: < <http://www.iea.org/publications/freepublications/publication/transition-to-sustainable-buildings.html>> (accessed 31.10.17)
- [10] O’Grady, A.M.; Lechowska, A.A; Harte, A.M. Quantification of heat losses through building envelope thermal bridges influenced by wind velocity using the outdoor infrared thermography technique. *Applied Energy* 108 (2017) 1038 - 1052
- [11] Taylor, T; Counsell, J; Gill, S. *Energy efficiency is more than skin deep: Improving construction quality control in new-building housing using thermography*. *Energy and Buildings* 66 (2013) 222-231
- [12] Cuerda, E; Pérez, M; Neila, J. *Façade typologies as a tool for selecting refurbishment measures for the Spanish residential building stock*. *Energy and Buildings* 76 (2014) 119-129
- [13] Tejedor, B; Casals, M; Gangoellés, M; Roca, X. *Quantitative internal infrared thermography for determining in-situ thermal behaviour of façades*. *Energy and Buildings* 151 (2017) 187-197
- [14] Albatici, R; Tonelli, A.M. *Infrared thermovision technique for the assessment of thermal transmittance value of opaque building elements on site*. *Energy and Buildings* 42 (2010) 2177-2183
- [15] Fokaides, P.A.; Kalogirou, S.A. *Application of infrared thermography for the determination of the overall heat transfer coefficient (U-Value) in building envelopes*. *Applied Energy* 88 (2011) 4358-4365
- [16] Asdrubali, F; Baldinelli, G; Bianchi, F. *A quantitative methodology to evaluate thermal bridges in buildings*. *Applied Energy* 97 (2012) 365-373

- [17] Dall'O, G; Sarto, L; Panza, A. *Infrared screening of residential buildings for energy audit purposes: results of a field test*. *Energies* 6 (2013), 3859-3878
- [18] Asdrubali, F; D'Alessandro, F; Baldinelli, G; Bianchi, F. *Evaluating in situ thermal transmittance of green buildings masonries –A case study*. *Case Studies in Construction Materials* 1 (2014) 53-59
- [19] Biddulph, P; Gori, V; Elwell, C.A.; Scott, C; Rye, C; Lowe, R; Oreszczyn, T. *Inferring the thermal resistance and effective thermal mass of a wall using frequent temperature and heat flux measurements*. *Energy and Buildings* 78 (2014) 10-16
- [20] Kylili, A; Fokaides, P.A.; Christou, P; Kalogirou, S.A. *Infrared thermography (IRT) applications for building diagnostics: A review*. *Applied Energy* 134 (2014) 531 -549
- [21] Taylor, T; Counsell, J; Gill, S. *Combining thermography and computer simulation to identify and assess insulation defects in the construction of building façades*. *Energy and Buildings* 76 (2014) 130-142
- [22] Fox, M; Coley, D; Goodhew, S; de Wilde, P. *Thermography methodologies for detecting energy related building defects*. *Renewable and Sustainable Energy Reviews* 40 (2014) 296-310
- [23] Gaspar, K; Casals, M; Gangoellis, M. *A comparison of standardized calculation methods for in situ measurements of façades U-value*. *Energy and Buildings* 130 (2016) 592-599
- [24] Nardi, I; Paoletti, D; Ambrosini, D; de Rubeis, T; Sfarra, S. *U-Value assessment by infrared thermography: A comparison of different calculation methods in a Guarded Hot Box*. *Energy and Buildings* 122 (2016) 211-221
- [25] Lehman, B; Ghazi Wakili, K; Frank, Th; Vera Collado, B; Tanner, Ch. *Effects of individual climatic parameters on the infrared thermography of buildings*. *Applied Energy* 110 (2013) 29-43

- [26] Tzifa, V; Papadakos, G; Papadopoulou, A.G.; Marinakis, V; Psarras, J. *Uncertainty and method limitations in a short-time measurement of the effective thermal transmittance on a building envelope using an infrared camera*. International Journal of Sustainable Energy (2014) 1-19
- [27] Albatici, R; Tonelli, A.M.; Chiogna, M. *A comprehensive experimental approach for the validation of quantitative infrared thermography in the evaluation of building thermal transmittance*. Applied Energy 141 (2015) 218-228
- [28] Nardi, I; Ambrosini, D; de Rubeis, T; Sfarra, S; Perilli, S; Pasqualoni, G. *A comparison between thermographic and flow-meter methods for the evaluation of thermal transmittance of different wall constructions*. Journal of Physics, Conference Series 655 (2015) 012007
- [29] Madding, R. *Finding R-values of stud frame constructed houses with IR thermography*. Proceedings of InfraMation (2008)
- [30] Cesaratto, P.G; De Carli, M. *A measuring campaign of thermal conductance in situ and possible impacts on net energy demand in buildings*. Energy and Buildings 59 (2013) 29-36
- [31] Ficco, G; Iannetta, F; Ianniello, E; d'Ambrosio, F.R.; Dell'Isola, M. *U-Value in situ measurement for energy diagnosis of existing buildings*. Energy and Buildings 104 (2015) 108-121
- [32] Rabadiya, A.V.; Kirar, R. *Comparative analysis of wind loss coefficient (wind heat transfer coefficient) for solar plate collector*. International Journal of Emerging Technology and Advanced Engineering (IJETA). ISSN 2250-2459, Volume 2, Issue 9, 2012
- [33] International Organization for Standardization, 2011. UNE EN ISO 13786:2011 Thermal performance of building components –Dynamic thermal characteristics –Calculation methods, 2011
- [34] Rossi, M; Rocco, V.M. *External walls design: The role of periodic thermal transmittance and internal areal heat capacity*. Energy and Buildings 68 (2014) 732 -740

- [35] O'Grady, A.M.; Lechowska, A.A.; Harte, A.M. Infrared thermography technique as an in-situ method of assessing heat loss through thermal bridging. *Energy and Buildings* 135 (2017) 20 – 32
- [36] FLIR Systems, 2015. FLIR TOOLS+ Software
- [37] Spain, 2006. Royal Decree 314/2006 approving the Spanish Technical Building Code CTE-DB-HE1. Available at: < <http://www.boe.es/boe/dias/2006/03/28/pdfs/A11816-11831.pdf> > (accessed 04.10.16)
- [38] International Organization for Standardization, 2012. UNE EN ISO 10456:2012 Building materials and products –Hygrothermal properties –Tabulated design values and procedures for determining declared and design thermal values, 2012
- [39] International Organization for Standardization, 2012. UNE EN ISO 6946:2012 Building components and building elements. Thermal resistance and thermal transmittance. Calculation method, 2012
- [40] International Organization for Standardization, 2008. ISO/IEC Guide 98-3:2008. Uncertainty of Measurement. Part 3: Guide to the Expression of Uncertainty in Measurement (GUM: 1995), 1998
- [41] Spain, 1979. Royal Decree 2429/1979 approving the Basic Building Norm on Thermal Conditions in Buildings NBE-CT-79. Available at: < <https://www.boe.es/boe/dias/1979/10/22/pdfs/A24524-24550.pdf> > (accessed 04.10.16)
- [42] IBM, 2017. SPSS Statistics v.24 Software
- [43] Kumar, A; Suman, B.M. *Experimental evaluation of insulation materials for walls and roofs and their impact on indoor thermal comfort under composite climate*. *Building and Environment* 59 (2013) 635-643

[44] Love, P. *Influence of project type and procurement method on rework costs in building construction projects*. Journal of Construction Engineering and Management 128 (2002) 18-29

[45] Forcada, N; Macarulla, M; Fuertes, A; Casals, M; Gangoells, M; Roca, X. *Influence of building type on post-handover defects in housing*. Journal of Performance of Constructed Facilities 26 (2012) 433-440

ACCEPTED MANUSCRIPT